Regular Article

ANALYTICAL AND BIOANALYTICAL CHEMISTRY RESEARCH

Published by the Iranian Chemical Society

Anal. Bioanal. Chem. Res., Vol. 9, No. 1, 73-83, January 2022.

MCR-ALS for Investigating the Effect of Adsorption on the Charging Current; Application for the Voltammetric Determination of Mefenamic Acid on a Glassy Carbon Electrode Modified with MWCNT and Poly L-Proline

Mehdi Moghtader, Morteza Bahram* and Khalil Farhadi

Department of Analytical Chemistry, Faculty of Chemistry, Urmia University, Urmia, Iran

(Received 23 March 2021 Accepted 9 August 2021)

This study represents the application of MCR-ALS for the separation of the different sources of variation in a series of the linear sweep voltammograms obtained from the oxidation of the mefenamic acid as a model analyte on a poly L-proline and MWCNT-modified GCE. Two types of faradaic currents including adsorption and diffusion were separated successfully and the effects of the accumulation time and the concentration of mefenamic acid were investigated on the variation of the charging current. The results showed that the contribution of the charging current on the measured signal decreases upon increasing the adsorption as a result of the blockage of the electrode active sites with the adsorbed species which is in agreement with the previous studies. The proposed methodology was employed for the voltammetric determination of mefenamic acid with enhanced figures of merit in real serum samples by removing the contribution of the charging current from the measured signal. The obtained results represent lower detection limit as 90 nM, wider linear range and higher sensitivity compared to the unprocessed and background-subtracted data.

Keywords: MCR-ALS, Charging current, Linear sweep voltammetry, Adsorption, Modified electrode

INTRODUCTION

An important factor that limits the performance of most voltammetric methods (especially Linear Sweep Voltammetry (LSV) and Cyclic Voltammetry (CV)) by restricting the sensitivity and detection limits is the presence of the charging current. This current originates from the formation of an electric double-layer on the surface of the electrode in addition to the redox reactions of the surface-attached functional groups, which cause a time-dependent capacitive current in the electrochemical measurements [1,2]. Change in potential, electrode surface area, or solution composition results in the flow of the charging current [3], and the type of the excitation signal, potential scan rate and the presence of adsorbed species affects its magnitude [4]. Adsorption causes the change in the composition of the electrode in the electrode/solution interface and any factor that controls this phenomenon, such as the time or bulk concentration of the adsorbed components, will affect the charging current [5-8]. Generally, two classes of methodologies have been employed to deal with the charging current and reduce its effect on the electrochemical measurements. The first class includes real-time techniques such as electrode modification, background subtraction, circuit design and improving the electrochemical instrumentation and invention of the sensitive electroanalytical methods like differential pulse and square wave voltammetric techniques [2,9-11]. The other class is the use of mathematical post-processing methods, which aim to separate the contribution of the different sources of variation in electrochemical signals including faradaic and charging currents. In this manner, different strategies like curve-fitting, Kalman filter, derivative techniques, Fourier transform, MCR-ALS, ITTFA, and ATLD were employed [12,13].

Although many electroanalytical methods suffer from

*Corresponding author. E-mail: m.bahram@urmia.ac.ir

the lack of linearity between the response and the bulk concentration of electroactive species as a result of different phenomena take place at electrode interface, the application of chemometrics techniques in electrochemistry, especially voltammetric methods, show an increasing trend during the last two decades by the development of instrumentation and mathematical analysis methods to improve the resolution power of electrochemical data or lower the detection limits [14-19]. MCR-ALS is a variant of MCR techniques for analysis and modeling of chemical data that uses an iterative algorithm to represent a bilinear description of data by decomposing the data matrix into a linear model of chemically-meaningful dyads by the implementation of diverse and application-oriented constraints to resolve the pure contribution of the components in two modes of an unresolved mixture data matrix or multiple augmented matrices. For a matrix D of the experimental voltammograms with each sample as a row of the matrix and the potentials on the columns, the MCR-ALS decomposition for a given number of components results in the product of a C matrix of the concentrations of components in different samples and a V matrix containing the pure signal of each component regarding the change in potentials (pure voltammograms) in addition to an error matrix E as Eq. (1):

$$D = CV^T + E \quad (1)$$

An initial estimation of either C or V is required to start the algorithm [14,20]. In case of linear sweep and cyclic voltammetry, this bilinear decomposition is only valid for the electrochemically inert or reversible systems in which the shape and position of the voltammograms do not undergo significant changes upon the change in the investigated parameters, including the potential scan rate. In addition, the currents should be linearly dependent on the concentration of the electroactive species present in the investigated system. On the other hand, if the peak potentials are shifted by the change in the investigated parameters, the obtained voltammetric data are not bilinear as is the case for many quasi-reversible and irreversible systems, else the bilinearity is remaining even for these systems and bilinear decomposition techniques can be applied [15,21-23].

There can be found several examples of the MCR-ALS applications for the decomposition of the electrochemical data in the literature [18,24-29]. Note that despite spectroscopy in which component is associated with pure chemical species in the solution, for electrochemical data, component must be associated with a single electrochemical process giving rise to a signal. In this manner, besides a component for each diffusion-controlled redox reaction, there will be other components for adsorbed species as well as the charging current [15]. Recently Hemmateenejad and coworkers employed MCR-ALS in a series of publications for electrochemical signal separation focused especially on chronoamperometry and investigated the effects of different parameters including the supporting electrolytes, ionic liquids and electrode material on the resolved charging and faradaic currents [2,3,23,30,31].

This work represents the use of the MCR-ALS for the chemometrics decomposition of the linear sweep voltammetric data for visualizing the effect of the analyte adsorption on the behavior of the charging current by changing the analyte concentration and the accumulation time as two effective parameters on the adsorption phenomenon. Linear sweep voltammetry was selected as the working method because it does not effectively removes the contribution of the charging current from the measured signal as other sensitive techniques like DPV or SWV[32]. The proposed method was employed for determination of Mefenamic acid (MFA), a nonsteroidal anti-inflammatory drug (NSAID), as a model analyte in real samples with the enhanced figures of merit by the removal of the resolved charging current from the measured signals on a modified glassy carbon electrode.

EXPERIMENTAL

Materials and Methods

MWCNT (>99% purity) was purchased from VCN Nano, Bushehr, Iran. L-proline (Merck, Germany) and MFA (Alborz bulk pharmaceutical Company, Saveh, Iran) were used as received. All other chemicals (Merck, Germany) were of analytical grade and used without further purifications. A stock solution of 0.01 M MFA was prepared by dissolving MFA in water using some droplets of NaOH solution. A 1.0 M phosphate-buffered saline (PBS

pH 8) was prepared and used. Standard solutions of MFA were prepared by diluting the stock MFA solution with PBS. Human serum samples of healthy volunteers were obtained from Imam Khomeini hospital (Urmia, Iran). Protein precipitation was performed by adding 3 ml of acetonitrile to 1 ml of serum sample and then centrifuged at 4000 rpm for 10 min. The supernatant was separated, diluted 10 times, and used as a real sample. Doubly distilled water (DDW) was used throughout the experiments.

Apparatus and Software

Electrochemical measurements were carried out using a SAMA500 electroanalyzer (Isfahan-Iran). A three-electrode system consisted of a platinum auxiliary electrode, an Ag/AgCl (sat. KCl) reference electrode and an unmodified glassy carbon electrode (GCE). A Metrohm-750 desktop pH-meter and Froilabo Velocity14-R desktop centrifuge (14000 rpm) were used. An Elma Elmasonic E60H ultrasonic bath was used when needed.

MCR-ALS calculations were performed in MATLAB 9.5 (MathWorks, Natick, MA, USA) using a freely available simple-to-use graphical user interface package on the web [www.cid.csic.es/homes/rtaqam/tmp/WEB_MCR/download/soft/mcr_toolbox2.zip]. Microsoft Excel 2016 was used to plot the curves and statistical calculations.

Electrode Preparation

The MWCNT was purified and functionalized according to earlier described methods with slight modifications [33-35]. The surface of the bare GCE was polished with emery paper (grades 800 and 1000) and alumina powder, then thoroughly rinsed with water, cleaned in an ultrasonic bath for 10 min and finally rinsed with DDW. An electrochemical cleaning step was also performed by scanning the potential in the ranges -0.5 V to 1.5 V at 100 mV s^{-1} scan rate in 0.5 M H_2SO_4 solution for 20 cycles and then rinsed with DDW. Appropriate amounts of the functionalized MWCNT were dissolved in DMF by sonication to obtain a 1 mg ml^{-1} suspension. 5 µl of this suspension was cast on the surface of the clean and dry electrode and allowed to dry for 2 h. As a previously reported procedure [36], electropolymerization of L-proline on the MWCNT/GCE was performed by cyclic voltammetry in a 0.1 M PBS (pH 8) containing 100 µM L-proline by scanning potential in the ranges -0.6 V to 1.8 V for 10 cycles at 100 mV s^{-1} then rinsed with DDW. The modified electrode was maintained in PBS (pH 7) when not in use.

Working Procedure

10 ml volumetric flasks were used to prepare experimental solutions. Proper amounts of stock MFA solution were transferred to the flask, 1 ml of 1.0 M PBS was added and then diluted to the mark by DDW. In case of real samples, 100 µl of the prepared serum sample was added before diluting to the mark. The surface of the working electrode was electrochemically cleaned before any experiment by cycling the potential in the ranges 0.0 -1.0 V in 0.1 M PBS (pH 8) for 10 cycles at 50 mV s^{-1}. Cyclic voltammograms of the experimental samples were recorded in the ranges 400-800 mV at 50 mV s^{-1} and arranged in a data matrix with as many rows as the number of experiments and columns equal to the number of potentials. Only forward scans (LSV experiments) were selected for MCR-ALS calculations in the ranges 500-700 mV. Except for mean-centered and background-subtracted data, no other pretreatments were performed.

RESULTS AND DISCUSSION

Voltammetric Characterization of the Modified Electrode

The electron transfer properties of the modified electrodes were characterized by CV. Figure 1a shows the cyclic voltammograms of bare GCE, MWCNT/GCE and poly L-pro/MWCNT/GCE in a 1.0 mM $K_3Fe(CN)_6/K_4Fe(CN)_6$ solution containing 0.1 M PBS (pH 8) at scan rate 50 mV s^{-1}. The peak-to-peak separation (ΔE_p) for bare GCE is 84 mV. Modification of bare GCE with MWCNTs results in an increase in peak currents and a decrease of ΔE_p to 79 mV. This suggests the increased surface area of the electrode after modification, but the electron transfer kinetics does not change significantly. Electropolymerization of L-proline on the MWCNT/GCE, leads to a slight decrease of peak currents compared to the

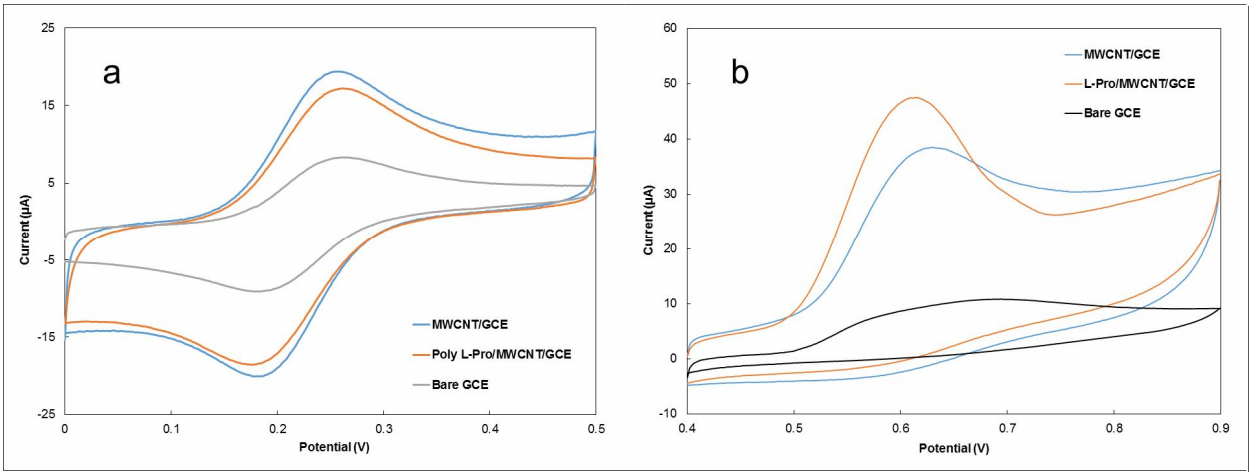

Fig. 1. Cyclic voltammograms of a) 1.0 mM $K_3Fe(CN)_6/K_4Fe(CN)_6$; b) 100 µM MFA in 0.1 M PBS pH 7, scan rate 50 mV s^{-1}, accumulation time 5 s at the surface of different electrodes.

MWCNT/GCE, probably due to the prevention of $[Fe(CN)_6]^{3-/4-}$ diffusion from solution to the surface of the electrode by the conducting polymer. In this case, ΔE_p increased to 86 mV.

Figure 1b shows an irreversible electrochemical behavior for electro-oxidation of 100 µM MFA in 0.1 M PBS (pH 8) at 50 mV s^{-1} on the modified electrodes. A broad oxidation peak at 694 mV was observed on bare GCE with I_{pa} equals to 10.8 µA. The anodic peak potential decreased to 629 and 615 mV for MWCNT/GCE and poly L-pro/MWCNT/GCE respectively, due to the catalytic effects of modifiers, while anodic peak currents increased significantly compared to bare GCE because of the higher electrode surface. This suggests the enhanced electrode reaction of the MFA on the modified electrodes. Also, the lower E_{pa} and higher I_{pa} on poly L-pro/MWCNT/GCE compared to MWCNT/GCE upon electro-oxidation of MFA, reveals better interaction of MFA with electrode surface in case of the poly L-pro/MWCNT/GCE probably due to the hydrogen bonding interaction between poly L-proline and MFA [37,38].

The effect of potential scan rate (υ) on the oxidation of 10 µM MFA in 0.1 M PBS (pH 8) on the fabricated sensor was studied by CV in the ranges 10-300 mV s^{-1} with 5 s of accumulation time and is depicted in Fig. 2a. By increasing the scan rate, no potential shifts were observed for the oxidation peaks of MFA. The plot of the peak current (I_{pa}) *vs*. the scan rate (υ) (Fig. 3a) is linear in the ranges 20 to 300 mV s^{-1} while for the square root of the scan rate ($\upsilon^{1/2}$) (Fig. 3b) two types of linear behaviors with different slopes are observed at the same range and this plot is not linear in the whole studied range. Figure 2b is the linear plot of $\log(I_p)$ *vs*. $\log(\upsilon)$ in the ranges 20-300 mV s^{-1}. For a fully diffusion-controlled electrode reaction, the slope of this relationship is theoretically 0.5 (dependent to the square root of the scan rate), while for an adsorption-controlled reaction, it is close to unity. The value of 0.9196 for the slope emphasizes the role of the adsorption against the diffusion in the evolution of the voltammetric signal for the oxidation of MFA on the surface of the modified electrode, while the role of the analyte diffusion cannot be ignored.

Figure 4a is the cyclic voltammograms for the pH-dependent oxidation of MFA in the pH ranges 6-11. Increasing the pH results in the shift of the oxidation peaks toward negative potentials, which indicates the ease of anodic reaction at lower concentrations of proton maybe due to the facilitated ionization of MFA regarding its pKa value. Optimal pH was selected as pH 8 for further experiments. Figure 4b shows the linear correlation of the anodic peak potential (E_{pa}) *vs*. pH with the regression equation of E_p = -0.0385pH + 0.8704 (R^2 = 0.9913). The slope of the equation (38.5 mV) indicates a two-electron

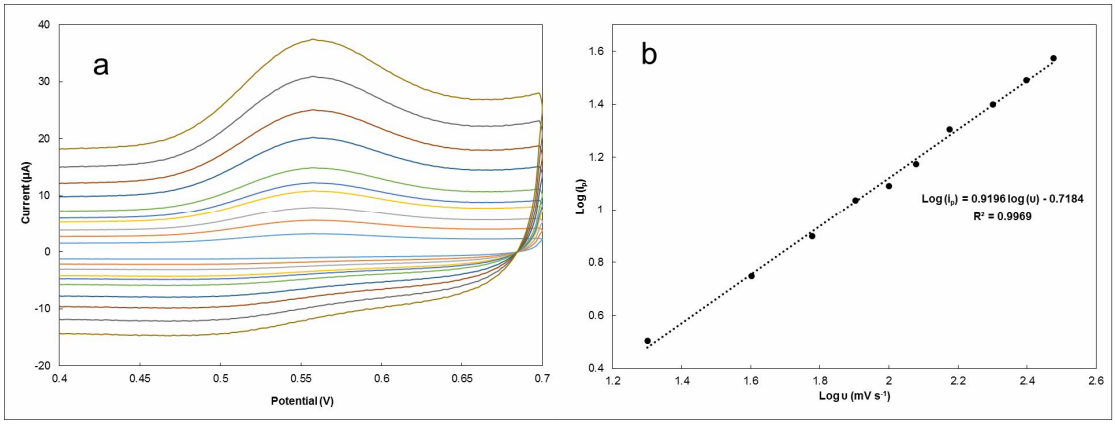

Fig. 2. a) Cyclic voltammograms for the oxidation of 10 µM MFA at different scan rates; b) dependence of the logarithm of peak current (log(I_p)) *vs.* logarithm of scan rate (logυ).

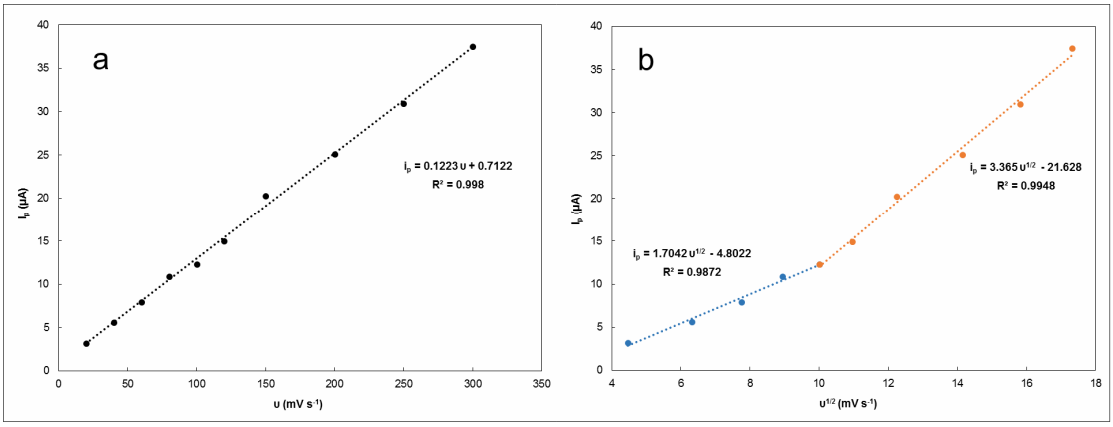

Fig. 3. Plots of a) I_p *vs.* scan rate (υ) b) I_p *vs.* square root of scan rate ($\upsilon^{1/2}$) for the oxidation of 10 µM MFA in 0.1 M PBS pH 8.

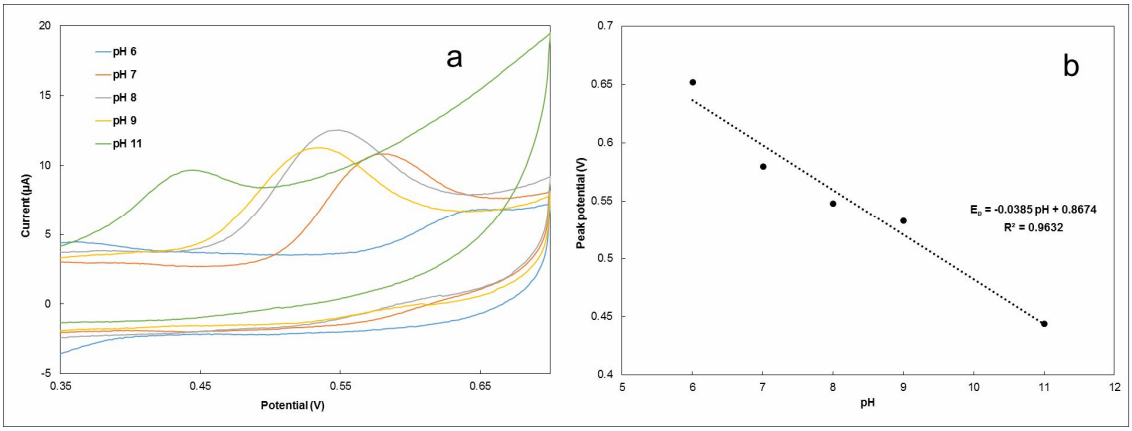

Fig. 4. a) Effect of pH on the oxidation of 10 µM MFA in 0.1 M PBS, scan rate 50 $mV.s^{-1}$, accumulation time 5 s; b) Influence of pH on the peak potential of MFA.

transfer reaction and the participation of unequal numbers of electrons and protons in the oxidation process [39].

Accumulation time is an important parameter in case of reactions in which adsorption takes place. This is because of the increased concentration of adsorbed species upon increasing its accumulation time and the subsequent increase in the sensitivity. The effect of this parameter was investigated for a 10 µM solution of MFA in 0.1 M PBS (pH 8) at 50 mV s^{-1} in the ranges 5-300 s which is depicted in Fig. 5. An optimal accumulation time of 120 s was selected for further experiments since no significant change in peak current was observed at higher accumulation times. Please insert Fig. 5

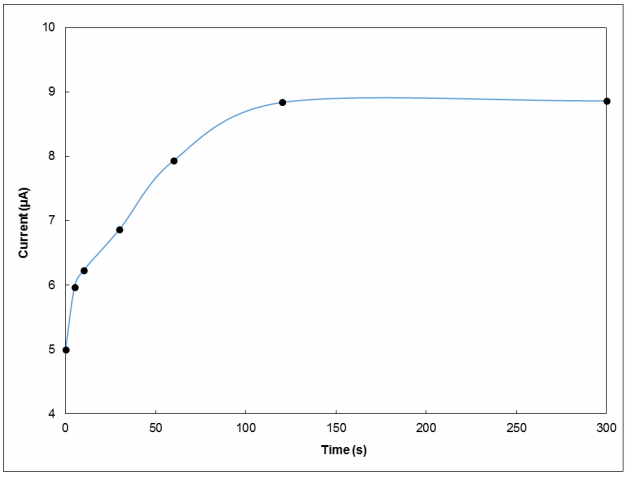

Fig. 5. Variation of the peak current with time, 10 µM MFA in 0.1 M PBS pH 8, scan rate 50 mV s^{-1}.

MCR-ALS Analysis of the Data

The first step in the decomposition of a data matrix by MCR-ALS is the correct estimation of the significant number of principal components. This is usually achieved by SVD-based rank analysis. Three types of datasets were used in this study. The first is a dataset containing ten repeated voltammograms of the blank samples containing only the supporting electrolyte (blank dataset), the second is a dataset containing seven voltammograms related to the optimization of accumulation time (accumulation time dataset) (Fig. 6), and the last one containing eleven voltammograms related to the calibration samples in addition to three real and three blank samples for LOD calculations (calibration dataset) (Fig. 7). Table 1 shows seven first eigenvalues for the analyzed datasets in addition to the statistical parameters of MCR-ALS decompositions. SVD analysis showed the presence of one, three and three principal components for blank, accumulation time and calibration datasets respectively, which can be attributed to the charging current for the blank dataset and charging current plus two types of faradaic current (diffusion and adsorption) for the other datasets regarding the definition of the component for voltammetric signals [2]. SIMPLISMA was used to obtain the initial estimates of linear sweep voltammograms for all datasets. Non-negativity constraint was applied on both modes of data matrices. In case of the calibration and accumulation time datasets, the resolved voltammogram of the blank dataset was used as an equality constraint for the pure contribution of the charging current.

Figure 8 shows the resolved current/time (*i-t*) profiles

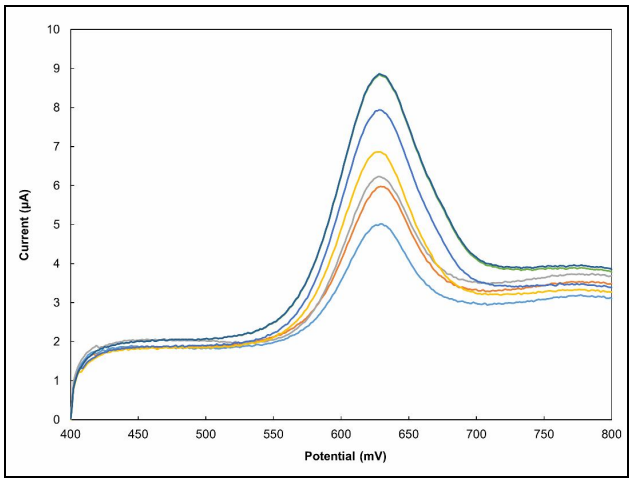

Fig. 6. Linear sweep voltammograms of the accumulation time dataset, 10 µM MFA in 0.1 M PBS pH 8, scan rate 50 mV s^{-1}.

and voltammograms (*i-V*) of the accumulation time dataset. The resolved voltammograms (Fig. 8a) show two types of faradaic processes for MFA oxidation with small differences in peak position. As the bulk concentration of the solution kept constant and the only difference among the voltammograms is related to the variation of the accumulation time, it is expected that the difference between the observed voltammograms arises from the adsorption of MFA on the surface of the electrode.

Table 1. SVD Analysis Results and MCR-ALS Model Parameters for Linear Sweep Voltammograms of Different Datasets

Parameters	Dataset name		
	Blank	Accumulation time	Calibration
Eigenvalues	108.1108	188.7932	349.9809
	2.7368	9.1362	46.9725
	1.1440	2.9947	21.1224
	0.6095	1.1098	3.6031
	0.5912	0.6798	1.9142
	0.4487	0.2547	1.4931
	0.4236	0.1562	0.6780
Number of iterations	12	10	5697
%Lack of fit (LOF)	2.9686	1.1332	2.2881
%Explained variance	99.9119	99.9872	99.9476

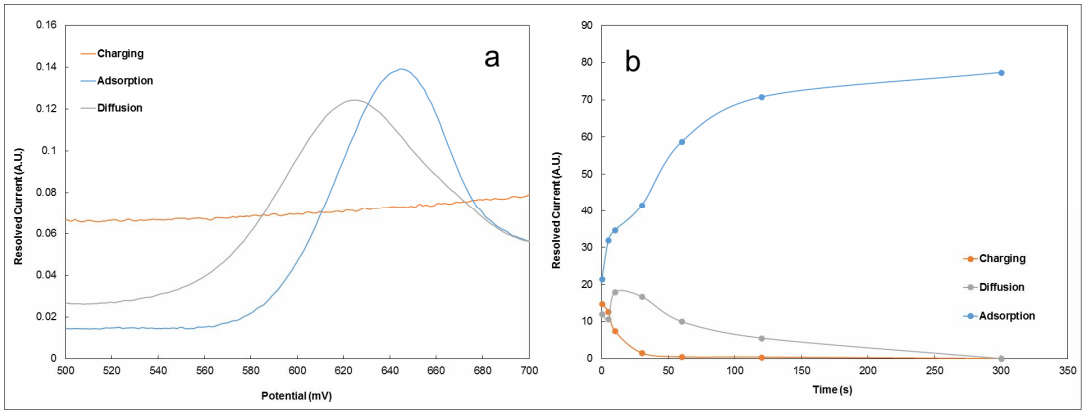

Fig. 8. Results of MCR-ALS for the linear sweep voltammograms of 10 µM MFA in 0.1 M PBS pH 8, scan rate 50 mV s^{-1} at different accumulation times including resolved a) linear sweep voltammograms b) current *vs*. time profiles.

Theoretically, this could result in the presence of post-peaks in the voltammograms in case of strong specific adsorption of reductant. Peak broadening also maybe occurs due to the small difference between the peak potentials of the adsorption- and diffusion-controlled processes if weak adsorption takes place [40-45]. The accepted procedure to distinguish the diffusion-controlled peaks from the adsorption-controlled ones is the change of the potential scan rate and investigate the linear behavior of the changes in the values of the peak currents as a function of the scan rate or the square root of the scan rate. However, this approach cannot be employed to obtain bilinear voltammetric data and investigate the behavior of the resolved faradaic currents upon the change of the scan rate because the irreversibility of the MFA oxidation leads to a subtle shift in peak potentials which restricts the use of bilinear data decomposition techniques like PLS and MCR-ALS due to the deviation from linearity in columns mode (voltammograms). Therefore we used the accumulation time data in which no peak potential shifts were observed

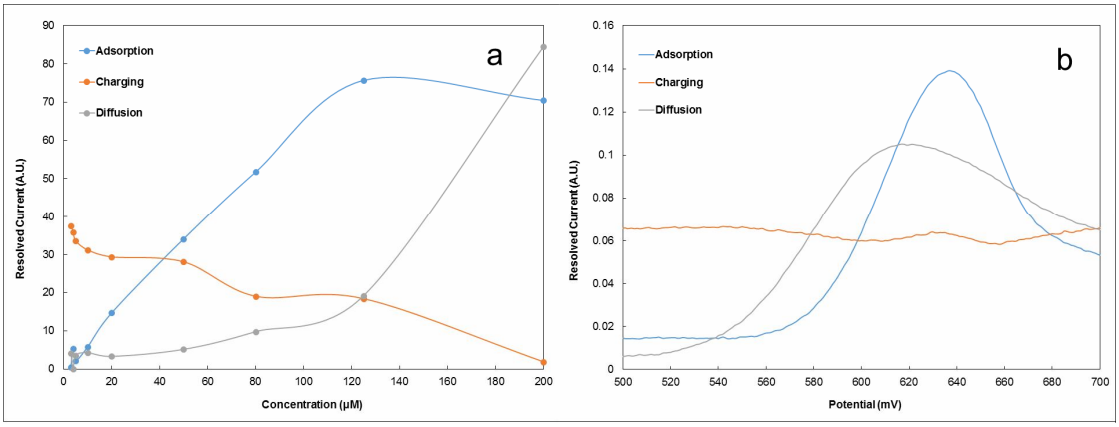

Fig. 9. Results of MCR-ALS for the linear sweep voltammograms of the different concentrations of MFA in 0.1 M PBS pH 8, scan rate 50 mV s^{-1}, accumulation time 120 s including resolved a) concentration profiles b) linear sweep voltammograms.

among the voltammograms upon the change in accumulation time. In this case, only the intensities of the faradaic currents were changed due to the variation in the extent of the adsorption, which leads to bilinear data. The investigation of the resolved *i-t* profiles in Fig. 8b clearly differentiates the two types of the faradaic currents. The resolved adsorption current shows an increase with the increase of the accumulation time as expected. The associated resolved voltammogram of this current also shows a higher peak potential (post-peak) compared to the associated voltammogram of the diffusion current, which is theoretically expected for an adsorbed species. Also, note to the high similarity between the evolution of the resolved adsorption current and the change in total unresolved peak current as a function of accumulation time depicted in Fig. 5.

On the other hand, the diffusion current decreases slightly as the adsorption current increases. This is due to the blockage of the active sites of the electrode surface upon the increase of the adsorption of MFA molecules that hinders the diffusion phenomenon and decreases the available active surface area of the electrode. The peak potential in the associated resolved voltammograms of this current is lower than that of adsorption, which is theoretically accepted for a diffusion-controlled current compared to the adsorption-controlled one. Another attractive point is the change of the charging current with the increase of the adsorption as expected. In lower accumulation times, the charging current is higher than the longer times in which the surface of the electrode is almost filled with the adsorbed species. The increase of the adsorption and the surface concentration of MFA compared to the small electrolyte ions and other impurities responsible for the evolution of the charging current leads to the decrease of the charging current at longer accumulation times due to a similar blockage effect of adsorbed MFA.

The proposed method was employed for the determination of MFA in real serum samples using different analyte concentrations at optimized experimental conditions. The obtained LSVs for calibration samples in the ranges 500-700 mV were arranged in a data matrix together with blank and spiked serum samples. The resolved concentration profiles (*i-C* curves) of the calibration samples are shown in Fig. 9a. Both faradaic currents (diffusion and adsorption) show increasing behavior upon increased concentrations of MFA. The variation in the resolved concentration profile of the adsorption current is higher than that of the diffusion current in the experimental concentration range until it reaches a plateau where the diffusion increased rapidly. The investigation of the charging current behavior regarding the concentration of MFA shows a similar trend compared to the accumulation

Table 2. Figures of Merit for the Proposed Method in Comparison with the other Methods

Parameters	Analysis method			
	Raw data	MCR-ALS	Background subtraction	Mean-centering
Regression equation	y = 0.0875x + 2.6464	y = 0.7568x + 2.0205	y = 0.0875x + 0.2312	y = 0.0253x + 0.2459
R^2	0.9999	0.9996	0.9989	0.9984
Linear range (μM)	5-200	0.5-200	8-200	20-200
LOD_{BL} (μM)[a]	1.60	0.09	1.60	6.83
LOQ_{BL} (μM)[a]	5.38	0.30	5.38	22.76
LOD_{CC} (μM)[b]	1.03	0.38	1.88	6.21
LOQ_{CC} (μM)[b]	3.45	1.16	6.27	20.72
Repeatability (%)	3.37	2.11	7.58	6.41

[a]Calculated from the standard deviation of the three repetitive blank measurements. [b]Calculated from the standard deviation of the calibration curve.

time dataset. As expected, a decrease in the charging current is observed by increasing the MFA concentration, and a constant charging current throughout the concentration range is not obtained. Although the overall behavior of the charging current in either datasets is decreasing, this trend is not fully similar because of the differences among the compositions of samples. Also similar resolved voltammograms (Fig. 9b) obtained compared to the accumulation time dataset (Fig. 8a).

A pseudo-univariate linear calibration curve was constructed using the summation of two resolved faradaic currents as the response of the electrode in the experimental concentration range. The LOD and LOQ (limit of quantitation) were calculated from Eq. (2) based on the standard deviation of three replicate measurements of the blank sample (s_{BL}) and the slope of the calibration curve (m). Also, the standard deviations of the calibration curves (s_{CC}) were calculated and used to obtain the LOD and LOQ values for comparison purposes [46]. The figures of merit for the proposed method were compared with the raw, mean-centered, and background-subtracted data and tabulated in Table 2.

$$LOD = 3s/m \qquad LOQ = 10s/m \qquad (2)$$

Although the application of the background subtraction causes an about 10-fold increase in the slope/intercept ratio by lowering the intercept of the regression equation, it results in higher LOD_{CC} and LOQ_{CC} values compared to raw data. The results for the mean-centering are even worse where lower sensitivity and higher LOD and LOQ were obtained. This is because of the higher values of s_{CC} compared to the s_{BL} which indicates some deviations from the regression line. A similar slope/intercept ratio compared to the background-subtracted data was obtained for the proposed method due to the 9-fold increase in the sensitivity. Lower detection and quantification limits and an increase in the linear range of the calibration curve suggests the improvement of the figures of merit upon application of MCR-ALS for electrochemical signal separation. A comparison of the figures of merits among some voltammetric studies for the determination of MFA was presented in Table 3.

The accuracy of the method was investigated by recovery measurements in serum samples spiked with known concentrations of MFA (Table 4). The recoveries ranged from 99.6-102.7%, suggesting the applicability of the proposed method in biological samples.

CONCLUSIONS

In this study the effect of the adsorption of electroactive

Table 3. Comparison of the Analytical Performance of the Different Modified Electrodes for MFA Determination

Electrode	Method	LOD	Linear range	Ref.
GCE	DPV	0.149	1-1000	[47]
IL/MWCNT/CHIT/GCE	DPV	1.23	2.0-650.0	[48]
MWCNTs-G/Ag	SWV	0.069	0.21-8.29	[49]
MWCNTs-CHT/GCE	DPV	0.66	4-200	[50]
BDDE	DPV	0.078	0.5-100	[51]
Poly L-Pro/MWCNT/GCE	LSV	0.09	0.5-200	Current work

Table 4. Analytical Results for Determination of MFA in Serum Samples

#Sample	Added (μM)	Found (μM)	Recovery (%)
1	0	<LOD	-
2	50.00	50.52	101.04
3	150.00	154.08	102.72
4	180.00	179.31	99.61

species on the behavior of the charging current was studied by changing the concentration and the accumulation time of the analyte as two effective parameters. MCR-ALS was employed to resolve a series of the measured linear sweep voltammograms to the pure contributions of the faradaic and charging currents. The visualization of the resolved *i-t* and *i-C* profiles showed the inverse variation of the charging current with the extent of the adsorption, which is in agreement with the previous studies. Two types of faradaic currents *i.e.*, adsorption and diffusion, were distinguished, separated and used for the determination of Mefenamic acid as a model analyte on the surface of a L-proline and MWCNT modified glassy carbon electrode with the enhanced figures of merit as a result of the exact removal of the contribution of the charging current.

REFERENCES

[1] A.R. Jalalvand, Sens. Bio-Sensing Res. 28 (2020) 100341.

[2] J. Tashkhourian, B. Hemmateenejad, S. Ahmadpour, E. Talebanpour Bayat, J. Electroanal. Chem. 801 (2017) 22.

[3] S. Ahmadpour, J. Tashkhourian, B. Hemmateenejad, J. Solid State Electrochem. 23 (2019) 3255.

[4] J.M. Diaz-Cruz, M. Esteban, C. Ariño, Exploratory Data Analysis, in: Chemom. Electroanal., Springer, 2019, pp. 33-67.

[5] R.M. Town, H.P. Van Leeuwen, J. Electroanal. Chem. 523 (2002) 1.

[6] D. Hobara, M. Ota, S.I. Imabayashi, K. Niki, T. Kakiuchi, J. Electroanal. Chem. 444 (1998) 113.

[7] S. Yoshimoto, M. Yoshida, S.I. Kobayashi, S. Nozute, T. Miyawaki, Y. Hashimoto, I. Taniguchi, J. Electroanal. Chem. 473 (1999) 85.

[8] S. Sander, T. Navrátil, L. Novotný, Electroanalysis. 15 (2003) 1513.

[9] M.D. Holtan, S. Somasundaram, N. Khuda, C.J. Easley, Anal. Chem. 91 (2019) 15833.

[10] A. Hermans, R.B. Keithley, J.M. Kita, L.A. Sombers, R.M. Wightman, Anal. Chem. 80 (2008) 4040.

[11] R.B. Keithley, P. Takmakov, E.S. Bucher, A.M. Belle, C.A. Owesson-White, J. Park, R.M. Wightman, Anal. Chem. 83 (2011) 3563.

[12] M. Jakubowska, Electroanalysis 23 (2011) 553.

[13] J. Tu, W. Cai, X. Shao, Analyst 139 (2014) 1016.

[14] A. Alberich, J.M. Díaz-Cruz, C. Ariño, M. Esteban, Analyst 133 (2008) 112.

[15] M.S. Díaz-Cruz, J. Mendieta, R. Tauler, M. Esteban, Anal. Chem. 71 (1999) 4629.

[16] M. Esteban, C. Ariño, J.M. Díaz-Cruz, TrAC-Trends Anal. Chem. 25 (2006) 86.

[17] M. Esteban, C. Ariño, J.M. Díaz-Cruz, Crit. Rev.

Anal. Chem. 36 (2006) 295.
[18] A.R. Jalalvand, H.C. Goicoechea, TrAC-Trends Anal. Chem. 88 (2017) 134.
[19] Y. Ni, S. Kokot, Anal. Chim. Acta 626 (2008) 130.
[20] A. De Juan, J. Jaumot, R. Tauler, Anal. Methods 6 (2014) 4964.
[21] A.R. Jalalvand, M. Roushani, H.C. Goicoechea, D.N. Rutledge, H.-W. Gu, Talanta. 194 (2019) 205.
[22] J. Díaz-Cruz, R. Tauler, B.S. Grabarić, M. Esteban, E. Casassas, J. Electroanal. Chem. 393 (1995) 7.
[23] A. Safavi, B. Hemmateenejad, F. Honarasa, Anal. Chim. Acta 766 (2013) 34.
[24] J.M. Díaz Cruz, J. Sanchís, E. Chekmeneva, C. Ariño, M. Esteban, Analyst 135 (2010) 1653.
[25] A.M. Garrigosa, J.M. Díaz-Cruz, C. Ariño, M. Esteban, Electrochim. Acta 53 (2008) 5579.
[26] S.M. Ghoreishi, M. Malekian, J. Electroanal. Chem. 805 (2017) 1.
[27] A. Khoobi, S.M. Ghoreishi, S. Masoum, M. Behpour, Bioelectrochemistry 94 (2013) 100.
[28] M. Meshki, M. Behpour, S. Masoum, Application of multivariate curve resolution alternating least squares method for determination of caffeic acid in the presence of catechin interference, Anal. Biochem. 473 (2015) 80.
[29] H. Abdollahi, M. Kooshki, Electroanalysis 22 (2010) 2245.
[30] B. Hemmateenejad, A. Safavi, F. Honarasa, J. Electroanal. Chem. 755 (2015) 221.
[31] S. Ahmadpour, J. Tashkhourian, B. Hemmateenejad, J. Electroanal. Chem. 871 (2020) 114296.
[32] A.J. Bard, L.R. Faulkner, Electrochemical Methods: Fundamentals and Applications, 2nd Edition, John Wiley & Sons, Incorporated, 2000.
[33] Y.S. Kim, J.Y. Oh, J.H. Kim, M.H. Shin, Y.C. Jeong, S.J. Sung, J. Park, S.J. Yang, C.R. Park, ACS Appl. Mater. Interfaces. 9 (2017) 17552.
[34] Z.Q. Gong, A.N.A. Sujari, S. Ab Ghani, Electrochim. Acta 65 (2012) 257.
[35] P. Kar, A. Choudhury, Sensors Actuators, B Chem. 183 (2013) 25.
[36] M.M. Charithra, J.G. Manjunatha, Mater. Sci. Energy Technol. 2 (2019) 365.
[37] S.K. Abdul Mudalip, M.R. Abu Bakar, P. Jamal, F. Adam, Ind. Eng. Chem. Res. 58 (2018) 762.
[38] V. Sasisekharan, Acta Crystallogr. 12 (1959) 897.
[39] S.D. Bukkitgar, N.P. Shetti, R.M. Kulkarni, S.T. Nandibewoor, RSC Adv. 5 (2015) 104891.
[40] H.P. Van Leeuwen, J. Buffle, M. Lovric, Pure Appl. Chem. 64 (1992) 1015.
[41] K.J. Aoki, J. Chen, Tips of Voltammetry, in: Voltammetry, IntechOpen, 2018.
[42] R. Abdel-Hamid, Monatshefte Für Chemie Chem. Mon. 119 (1988) 429.
[43] N. Kurapati, P. Pathirathna, R. Chen, S. Amemiya, Anal. Chem. 90 (2018) 13632.
[44] R.H. Wopschall, I. Shain, Anal. Chem. 39 (1967) 1514.
[45] D. Pletcher, R. Greff, R. Peat, L.M. Peter, J. Robinson, Instrumental Methods in Electrochemistry. Elsevier, 2001.
[46] J. Miller, J.C. Miller, Statistics and Chemometrics for Analytical Chemistry, Pearson Education, 2018.
[47] M.D. Tezerjani, A. Benvidi, M. Rezaeinasab, S. Jahanbani, M.M. Ardakani, J. Serbian Chem. Soc. 82 (2017) 1273.
[48] S. Kianipour, A. Asghari, IEEE Sens. J. 13 (2013) 2690.
[49] A.B. Moghaddam, A. Mohammadi, S. Mohammadi, Pharm. Anal Acta 3 (2012) 2.
[50] A. Babaei, M. Afrasiabi, M. Babazadeh, Electroanalysis 22 (2010) 1743.
[51] B.B. Petković, M. Ognjanović, M. Krstić, V. Stanković, L. Babincev, M. Pergal, D.M. Stanković, Diam. Relat. Mater. 105 (2020) 107785.